STUDY OF OZONE CONCENTRATION IN NORTH MADAGASCAR

MAXWELL Djaffard[1], DONA Victorien Bruno[1], RAKOTOVELO Geoslin[1], RATIARISON Adolphe Andriamanga[2]

[1]*Laboratory of Applied Physics and Renewable Energies, Mahajanga University, Madagascar*
[2]*Laboratory of Atmospheric, Climate and Ocean Dynamics, University of Antananarivo, Madagascar*

ABSTRACT

This article presents the study of ozone concentrations in the northern part of Madagascar, delimited by latitudes -12 ° to -18 ° and longitudes 43 ° to 51. The study of the evolution of the annual averages of theozone's concentrations showed the absence of significant trend according to the Mann-Kendall test.
The study area can be subdivided into three regions with respect to the 0h ozone concentration and four regions with respect to ozone 6h, 12h and 18h according to the study by principal component analysis.
The prediction of the evolution of the ozone concentration by the ARIMA method shows that some regions would know a constant or decreasing concentration and others would have a variable concentration that is almost periodic.

Keyword: *ozone, climatological mean, anomaly, trend, Mann-Kendall test, Principal Component Analysis, ARIMA*

1. INTRODUCTION

In the stratosphere, ozone is an essential gas. The ozone layer absorbs the UV radiation (240 to 320 nm) and thus protects the organisms against this harmful short wavelength radiation. In the troposphere, ozone absorbs radiation in the field of far infrared (between 4 and 40 µm), it is both a pollutant and a greenhouse gas that would have a radiative forcing of 0.35 $W.m^{-2}$ on average according to the IPCC.
Indeed, an increase in the concentrations of greenhouse gases in the troposphere leads to a warming in this layer but a cooling in the stratosphere. This decrease in stratospheric temperatures leads to a change in the rates of major chemical reactions: those depleting the ozone layer are slower, changing the concentrations of ozone in the stratosphere. Because of the faster transport of tropical air masses at higher latitudes, there is less time for ozone-depleting reactions to occur there. As a result, there would be an increase in the concentration of ozone in the middle and high latitudes. But what about tropical regions?
Figure 1 represents the study area located in the northern part of Madagascar. It is delimited by latitudes -12 ° to -18° and longitudes 43 ° to 51 °.

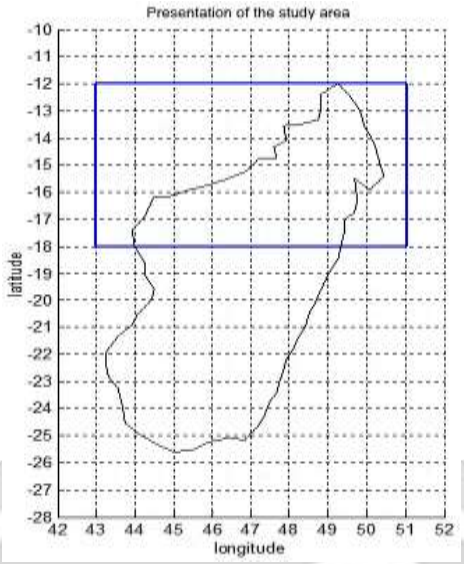

Figure 1: representation of the study area

2. METHODOLOGIES

2.1 Data

The data (vertically integrated ozone) are from ECMWF for the period 1979-2016, with spatial resolution 1 ° x1 °.

2.2 Methods

The methodology applied is to use:

- the Mann-Kendall test to detect the presence of trends within a time series in the absence of any seasonality or other cycles. The calculated statistic is defined by:

$$S=\sum_{i=1}^{n-1}\sum_{j=i+1}^{n}\operatorname{sgn}\left[\left(y_j-y_i\right)\left(x_j-x_i\right)\right] \text{ where } \operatorname{sgn}(X)=\begin{cases}+1 \text{ if } X>0\\ 0 \text{ if } X=0\\ -1 \text{ if } X<0\end{cases}$$

Mann (1945) and Kendall (1975) demonstrated that:

$$\begin{cases}E(S)=0\\ Var(S)=\dfrac{n(n-1)(2n+5)}{18}\end{cases}$$

If there are ex-aequo in the series, the variance of S is corrected as follows:

$$Var(S)=\frac{1}{18}\left[n(n-1)(2n+5)-\sum_{p=1}^{g}t_p\,(p-1)(2p+5)\right] \text{ where } t_p \text{ is the number of equalities involving p values}$$

As soon as the sample contains about a dozen data, the law of Z-test statistics can be approached by a centered-reduced gaussian.

$$Z=\begin{cases}\dfrac{S-1}{(Var(S))^{\frac{1}{2}}} & \text{if S>0}\\ 0 \text{ si S=0} & \\ \dfrac{S+1}{(Var(S))^{\frac{1}{2}}} & \text{if S<0}\end{cases}$$

If we have a sequence of observations $x_1, x_2, \ldots, x_n$ for which we make the two hypotheses:

$$\begin{cases}\text{Hypothesis null } H_0\text{: observations } x_i \text{ are randomly ordered, no trend}\\ \text{Alternative Hypothesis } H_1\text{: Observations } x_i \text{ shows increasing or decreasing trend}\end{cases}$$

The trend of the observation sequence is statistically significant when the p-value of the test is less than 5%. **[1]**

- **Normalized Principal Components Analysis**, which is a factorial dimension reduction method for the statistical exploration of complex quantitative data. This method is widely used in the analysis of climatological data. **[2], [3], [4], [5]**

  - For two statistical series $k = (x_k, n_k)$ and $h = (x_h, n_h)$ of the same size n with a time depth of several years, the linear correlation coefficient is given by:

$$r(k,h) = \frac{1}{n}\sum_{i=1}^{n}\left(\frac{x_{ik}-\bar{x}_k}{s_k}\right)\left(\frac{x_{ih}-\bar{x}_h}{s_h}\right) \quad \text{where} \quad \begin{cases}\bar{x}_k\text{: mean of k}\\ s_k\text{: standard deviation of k}\end{cases} \quad \begin{cases}\bar{x}_h\text{: mean of h}\\ s_h\text{: standard deviation of h}\end{cases}$$

  - Data matrix:

Iinitial data table

$$T = \begin{pmatrix} v_{11} & v_{21} & \cdots & v_{1(p-1)} & v_{1p} \\ v_{21} & v_{22} & \cdots & v_{2(p-1)} & v_{2p} \\ \vdots & \vdots & \cdots & \vdots & \vdots \\ v_{(n-1)1} & v_{(n-1)2} & \cdots & v_{(n-1)(p-1)} & v_{(n-1)p} \\ v_{n1} & v_{n2} & \cdots & v_{n(p-1)} & v_{np} \end{pmatrix}$$

Cloud point center of gravity

$$G = \begin{pmatrix} x_{G1} = \dfrac{\sum_{i=1}^{n} v_{i1}}{n} \\ \vdots \\ x_{Gp} = \dfrac{\sum_{i=1}^{n} v_{ip}}{n} \end{pmatrix}$$

Choosing G as the origin leads to the reduced data center table

$$T_{cr} = \begin{pmatrix} \dfrac{v_{11}-x_{G11}}{s_1} & \dfrac{v_{21}-x_{G21}}{s_2} & \cdots & \dfrac{v_{1(p-1)}-x_{G1(p-1)}}{s_{(p-1)}} & \dfrac{v_{1p}-x_{G1p}}{s_p} \\ \dfrac{v_{21}-x_{G21}}{s_1} & \dfrac{v_{22}-x_{G22}}{s_2} & \cdots & \dfrac{v_{2(p-1)}-x_{G2(p-1)}}{s_{(p-1)}} & \dfrac{v_{2p}-x_{G2p}}{s_p} \\ \vdots & \vdots & \cdots & \vdots & \vdots \\ \dfrac{v_{(n-1)1}-x_{G(n-1)1}}{s_1} & \dfrac{v_{(n-1)2}-x_{G(n-1)2}}{s_2} & \cdots & \dfrac{v_{(n-1)(p-1)}-x_{G(n-1)(p-1)}}{s_{(p-1)}} & \dfrac{v_{(n-1)p}-x_{G(n-1)p}}{s_p} \\ \dfrac{v_{n1}-x_{Gn1}}{s_1} & \dfrac{v_{n2}-x_{Gn2}}{s_2} & \cdots & \dfrac{v_{n(p-1)}-x_{Gn(p-1)}}{s_{(p-1)}} & \dfrac{v_{np}-x_{Gnp}}{s_p} \end{pmatrix}$$

Reduced centered coordinates of the individual u_i:

$$X_{cri} = \begin{pmatrix} \frac{v_{i1} - x_{Gi1}}{s_1} \\ . \\ . \\ . \\ \frac{v_{ip} - x_{Gip}}{s_p} \end{pmatrix}$$

Total inertia of the cloud of individuals :

$$I_G = \frac{1}{n}\sum_{i=1}^{n}\sum_{j=1}^{p}\left(\frac{v_{ij} - x_{Gij}}{s_j}\right)^2 = \sum_{j=1}^{p}\left(\frac{1}{n}\sum_{i=1}^{n}\left(\frac{v_{ij} - x_{Gij}}{s_j}\right)^2\right) = \sum_{j=1}^{p}\left(\mathrm{r}\left(v_{ij}\right)\right)$$

Covariance matrix:

$$R = \begin{pmatrix} r(v_{11}) & r(v_{12}) & . & . & . & r(v_{1(p-1)}) & r(v_{1p}) \\ r(v_{21}) & r(v_{22}) & . & . & . & r(v_{2(p-1)}) & r(v_{2p}) \\ . & . & . & . & . & . & . \\ . & . & . & . & . & . & . \\ . & . & . & . & . & . & . \\ r(v_{(p-1)1}) & r(v_{(p-1)2}) & . & . & . & r(v_{(p-1)(p-1)}) & r(v_{(p-1)p}) \\ r(v_{p1}) & r(v_{p2}) & . & . & . & r(v_{p(p-1)}) & r(v_{pp}) \end{pmatrix} = \begin{pmatrix} 1 & . & . & . & . & . \\ . & 1 & . & . & . & . \\ . & . & 1 & . & . & . \\ . & . & . & 1 & . & . \\ . & . & . & . & 1 & . \\ . & . & . & . & . & 1 \end{pmatrix}$$

$$\text{so } trace(R) = p = I_G$$

- Eigenvalues and eigenvectors :

$$T_{cr}(V) = \lambda V \text{ where } \begin{cases} \lambda : \text{ eigenvalue} \\ \mathrm{V} : \text{eigenvector} \end{cases}$$

Axes Δ_i passing through G and minimum inertia have for vector director eigenvectors V_i associated with eigenvaluess λ_i such as

$$I_G = \sum_{i=1}^{p}\lambda_i$$

- Selection of the principal axes to be chosen

$$\sum_{i=1}^{p}\lambda_i = p \Rightarrow \overline{\lambda} = \frac{\sum_{i=1}^{p}\lambda_i}{p} = 1 \text{ therefore we can not consider as significant that the } \lambda_i \geq 1$$

By Kaiser's empirical criterion, by centering and reducing the data, we retain the principal components corresponding to eigenvalues greater than 1. **[6]**

- Quality of representation of an individual u_i on an axis Δ_k

The parameter $cos^2\theta$ is used to characterize the quality of representation (qlt) on an axis**. [6]**

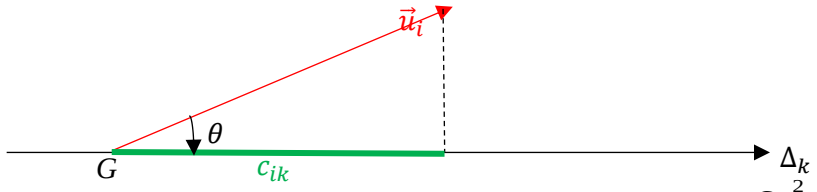

$$qlt_k(u_i) = \cos^2(\theta) = \frac{c_{ik}^{\ 2}}{\left\|\overrightarrow{Gu_i}\right\|^2}$$

$$\left\|\overrightarrow{Gu_i}\right\|^2 = \sum_{k=1}^{p} c_{ik}^{\ 2}$$

The closer qlt_i is to 1, the better it is represented.
The closer qlt_i is to 0, the more it is misrepresented. **[7]**

Quality of representation of variables**. [2], [3], [4]**
On a factorial plane defined by two pricipal axes :

- a variable close to the correlation circle is well represented in this plane;
- a variable close to the origin of the correlation circle is poorly represented in this plane.

- **the autoregressive model - moving mean**

➢ **ARMA**(p, q) process **[8], [9]**

The autoregressive - moving mean (ARMA), is characterized by a p parameter of the autoregressive part and a q parameter of the moving mean part. An ARMA(p, q) process checks the equation:

$$X_t = \phi_1 Xt\text{-}1 + ... + \phi_p X_{t-p} + E_t + \theta_1 E_{t-1} + ... + \theta_q E_{t-q} \text{ so } \Phi(B)X_t = \Theta(B)E_t.$$

The treatment of a such process is complex. It can be shown, however, that its autocorrelations and partial autocorrelations are depreciated functions tending towards 0 in absolute value at exponential speeds.
Analysis of correlograms is one of the preferred tools in model identification.

➢ ARIMA(p, d, q) model

A process X_t admits a polynomial trend of degree d, the differentiated process d times is stationary:

$$Y_t = \Delta^d X_t = (I\text{-}B)^d X_t.$$

The ARIMA model comes down to applying an ARMA model on the differentiated process:

$$Y_t = \text{ARMA}(p, q) \Leftrightarrow X_t = \text{ARIMA}(p, d, q).$$

The equation of an ARIMA(p, d, q) model is therefore given by:

$$\Phi(B)Y_t = \Theta(B)E_t \Leftrightarrow \Phi(B)\Delta^d X_t = \Theta(B)E_t$$

where Φ and Θ are two polynomials of respective degrees p and q. The 'I' of ARIMA means 'integrates' as a reciprocal of differentiation.
Degree d is not generally known. To determine it we can act by trial and error or resort to stationarity tests: since an ARMA process (p, q) is stationary, we try to accept the hypothesis of stationarity for the process $Yt = \Delta^d X_t$. In general, we refer to a parsimony principle and look for the minimum satisfying value of d.

3. RESULTS AND DISCUSSIONS

3.1 Climatological mean of ozone concentrations from 1979 to 2016 in the study area

Figure 2 shows the daily and monthly climatological mean curves of ozone concentrations at 0h, 6h, 12h and 18h in the study area.

In **Figure 2-a**:

- The maximum daily climatological mean ozone concentration is 6.016 $x10^{-3}$ $kg.m^{-2}$ (mean ozone concentrations 6h of October 22) and its minimum is 5.319$x10^{-3}$ $kg.m^{-2}$ (mean ozone concentrations of June 14).
- The daily climatological mean of the 6h ozone concentration is always higher than other measurements.
- From 151st to 304th day of the year ozone concentrations 18h and 0h are below 6h and 12h.

In **Figure 2-b**:

- The maximum monthly climatological mean ozone concentration is 6.012 x10^{-3} kg.m^{-2} (mean ozone concentrations 6h in October) and its minimum is 5.378 x10^{-3} kg.m^{-2} (mean of 18h ozone concentrations in June).
- The monthly climatological mean of the 6h ozone concentration is always higher than other measurements.
- From April to October the monthly climatological mean of the ozone concentration 12h is higher than the monthly climatological mean of the ozone concentration 18h and 0h.
- In the months of December and January the monthly climatological mean of the ozone concentration 12h is lower than the monthly climatological mean of the ozone concentration 18h and 0h.
- From August to April the monthly climatological mean of the ozone concentration 0h is lower than that of 18h.
- From May to July the monthly climatological mean of the ozone concentration 0h is higher than that of 18h.

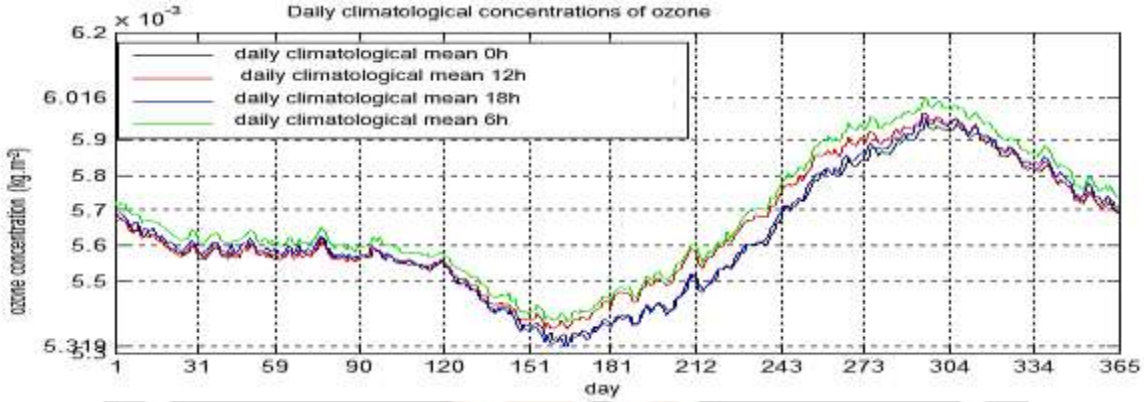

Figure 2-a

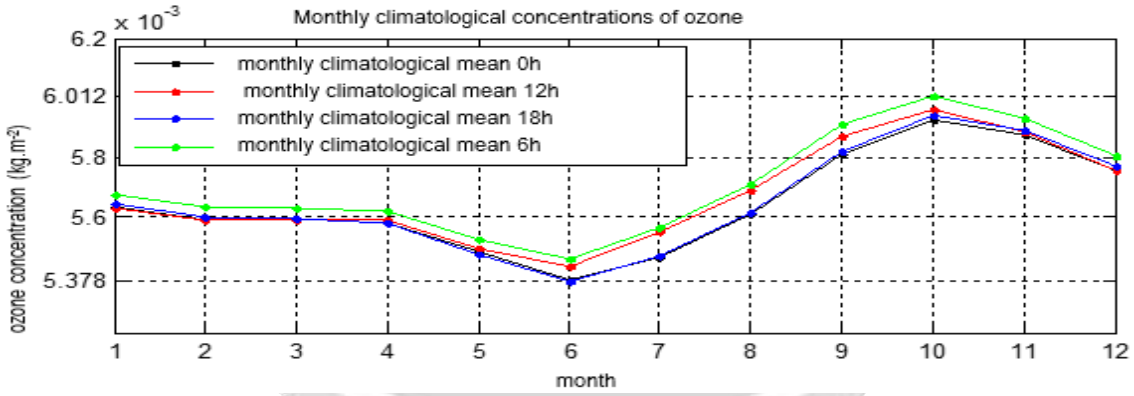

Figure 2-b

Figure 2 : variation of the daily and monthly climatological mean of ozone concentrations

3.2 Evolution of annual mean ozone concentrations since 1979 to 2016

Figure 3 shows the evolution of the annual mean ozone concentrations. The dashed lines represent the trend lines.

The annual average ozone concentration was maximum in 2000 (5.916x10^{-3} kg.m^{-2}) and minimum in 2005 (5.351x10^{-3} kg.m^{-2}).

The trend lines of the evolution of the ozone concentration for the different measurements are of low negative slope. So there is a general downward trend in ozone concentration over the study period. The Mann-Kendall test gives p-values well above 0.05 (p_value6h = 0.1997, p_value12h = 0.3926, p_value18h = 0.8406, p_value0h = 0.8015), the trend is therefore not significant.

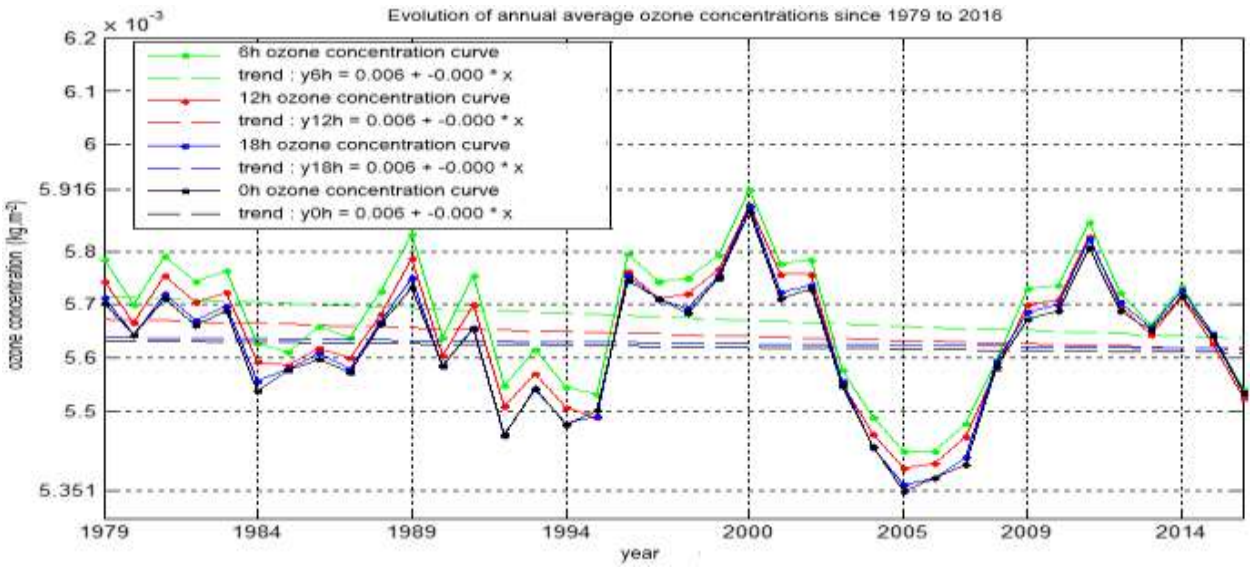

Figure 3 : curves and trend lines of annual average ozone concentrations

3.3 Annual anomaly of ozone concentration from 1979 to 2016

Figure 4 shows the annual anomaly of ozone concentrations for the different measurements. The study period is characterized by an almost periodic alternation of surplus and deficit of ozone concentrations :

- an alternation of surplus and deficit of almost four-year period between 1979 and 1995;
- an alternation of surplus and deficit of almost six-year period between 1996 and 2014.

The greatest excess of ozone concentration ($2.56x10^{-4}$ $kg.m^{-2}$) occurred in 2000 observed for the 18h ozone concentration.

The greatest deficit in ozone concentration ($-2.7x10^{-4}$ $kg.m^{-2}$) occurred in 2005 observed for ozone concentration 0h.

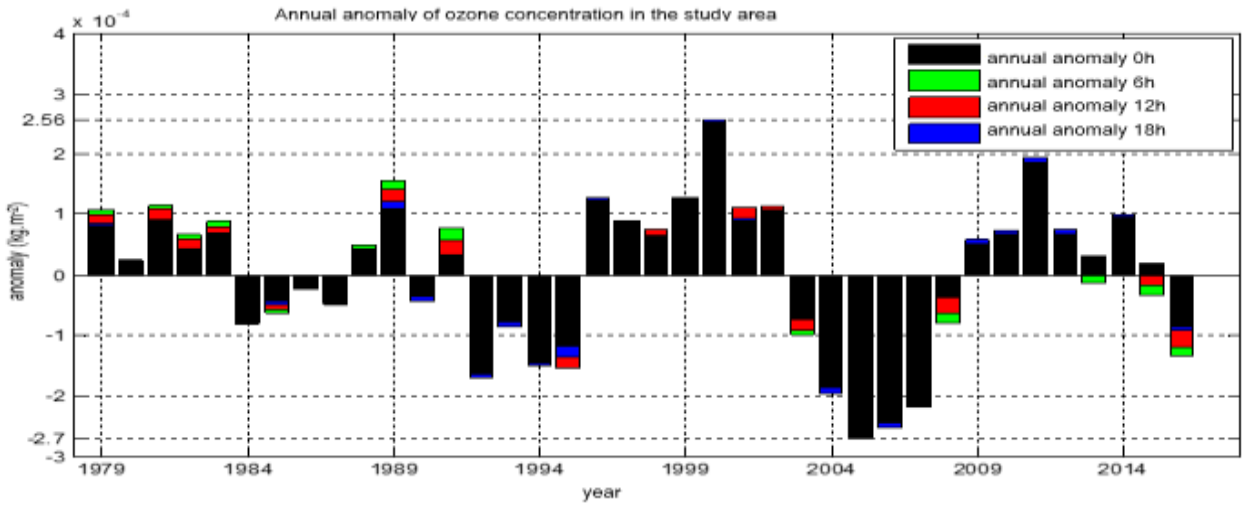

Figure 4 : annual anomaly of ozone concentration from 1979 to 2016

3.4 Principal Components Analysis results

In the principal component analysis, all ozone concentrations at each latitude and longitude intersection point in the study area were selected as individuals with spatial resolution of 1 ° x 1 ° and variables the 12 months of the year. Which gives 7 rows according to the latitude and 9 rows according to the longitude. There are 63 intersection points representing individuals. (**Figure 5**)

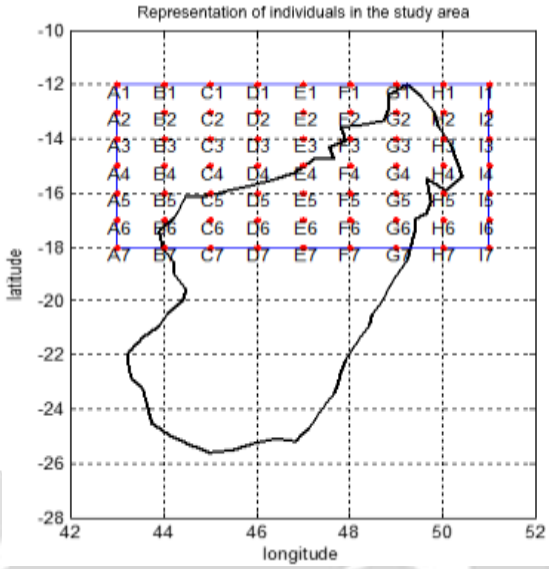

Figure 5 : representation of individuals in the study area

3.4.1 Choice of number of axis to be retained

To study the behavior of each individual vis-à-vis others, the Kaiser criterion and the elbow criterion allow to keep the factorial axes F1 and F2. These two axes explain more than 98% of the total inertia (98.35% for the 0h ozone concentration (**Figure 6-a**), 98.26% for the 6h ozone concentration (**Figure 6-b**), 99.03% for the 12h ozone concentration (**Figure 6-c**) and 98.49% for the 18h ozone concentration (**Figure 6-d**)).

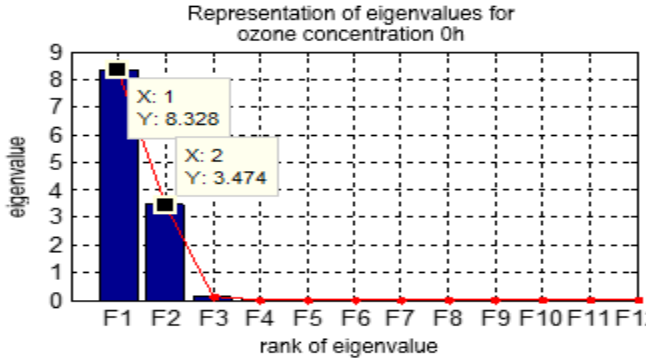

Figure 6-a

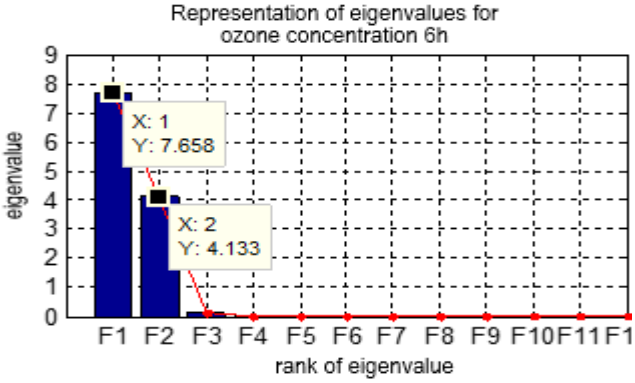

Figure 6-b

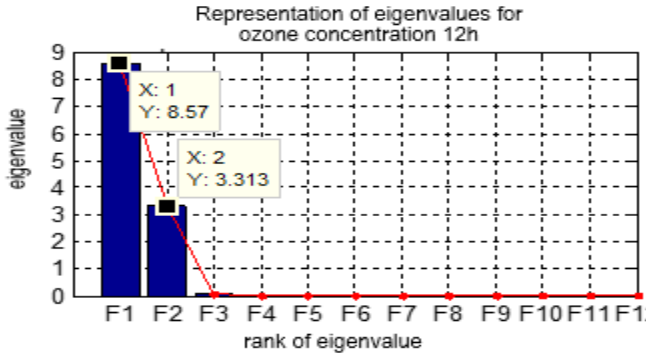

Figure 6-c

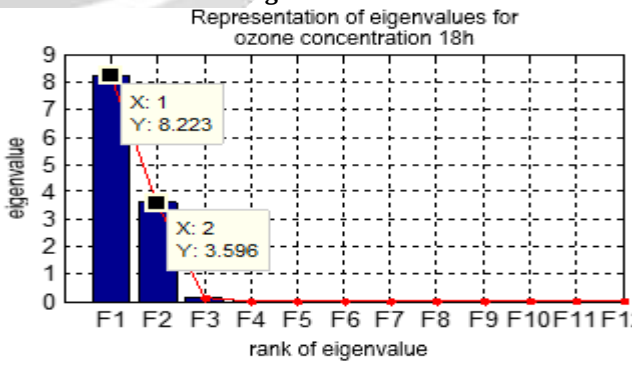

Figure 6-d

Figure 6 : representation of eigenvalues for ozone concentrations

3.4.2 Projections of variables on the factor plane F1-F2

Figure 7 shows the projection of the variables in the factorial plane F1-F2.

- All variables are well represented in the F1-F2 plane.
- The months of January, June, July and August are positively correlated with the F1 axis, which explains more than 63% of the total inertia of the scatter plot. These months are low ozone concentrations as shown in **Figure 2-b**. The F1 axis represents the months of low ozone concentrations (**Figures 7-a, 7-b, 7-c** and **7-d**).
- The months of September, October and November are positively correlated with the F2 axis, unlike in April and May. The F2 axis therefore opposes the months of high ozone concentrations and months of low ozone concentrations (**Figures 7-a, 7-b, 7-c** and **7-d**).

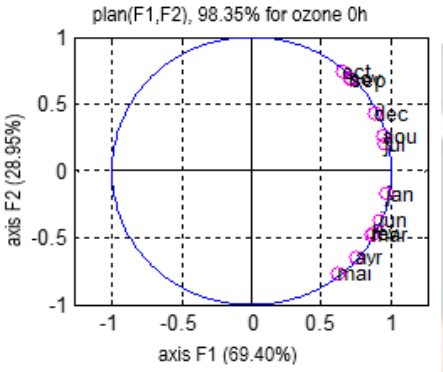

Figure 7-a

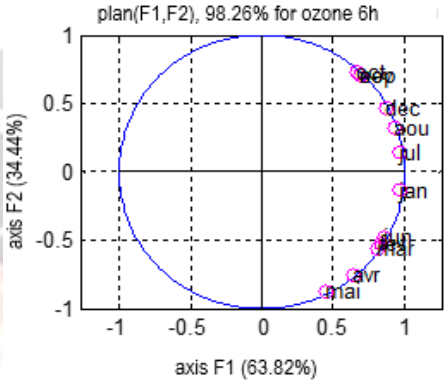

Figure 7-b

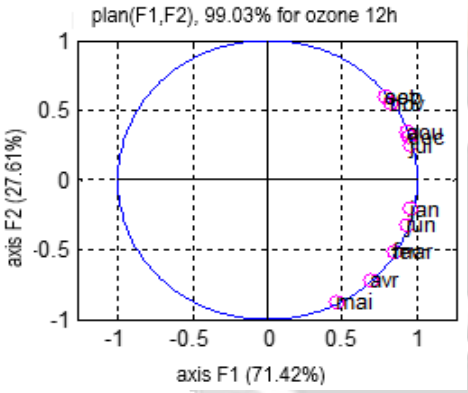

Figure 7-c

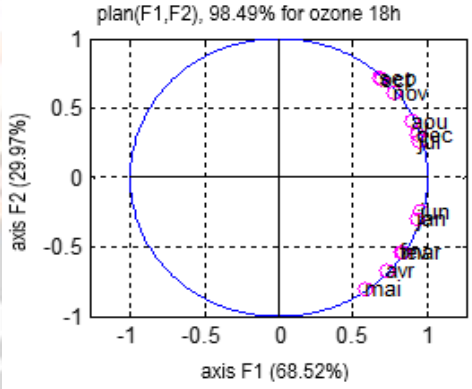

Figure 7-d

Figure 7 : projection of variables in the factorial plane F1-F2.

3.4.3 Projections of individuals on the factorial plane F1-F2

Figure 8 shows the projection of individuals in the factorial plane F1-F2.

- On **Figure 8-a**, for ozone concentration 0h :

- Individual A7 contributes most to the construction of the F1 axis. This individual is of low ozone concentration for all measurements during January, June, July and August, taking into account the correlation of the variables with the F1 axis.

- The F1 axis opposes individuals G3 and G4 to individual A7. These individuals have higher ozone concentrations for all measurements in January, June, July and August than individuals A7.

- On **Figure 8-b, 8-c** and **8-d** for ozone concentrations 6h, 12h and 18h :

  Individuals E7 and F7 contribute the most to the preparation of the F2 axis for the 6h, 12h and 18h ozone concentrations. These individuals have higher concentrations of ozone 6h, 12h and 18h during the months of September, October and November

- Other individuals have no particular behaviour with respect to ozone concentrations.

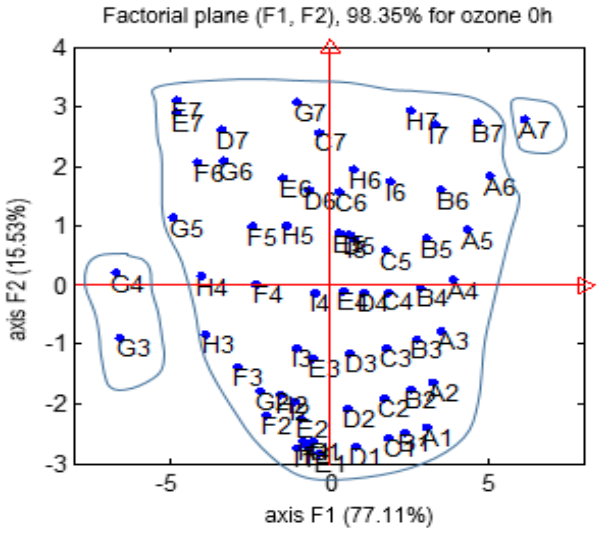

Figure 8-a

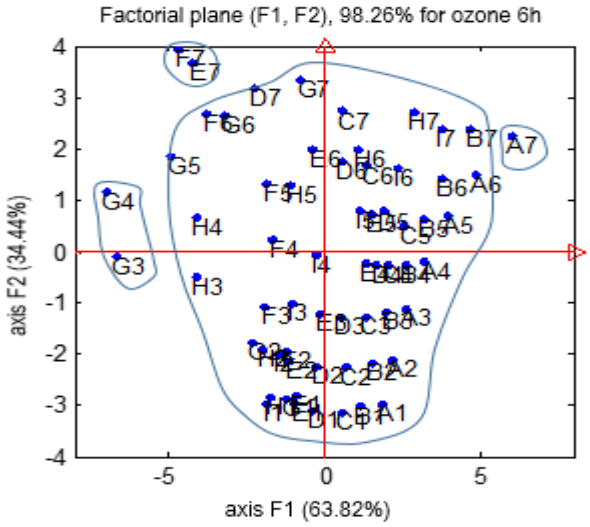

Figure 8-b

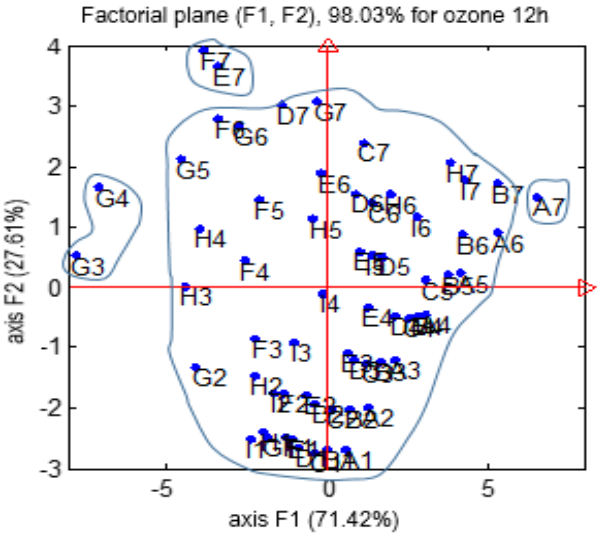

Figure 8-c

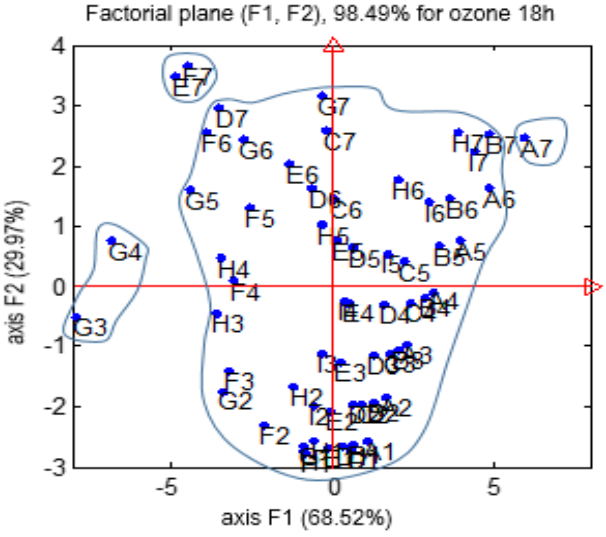

Figure 8-d

Figure 8 : projection of individuals on the factorial plane F1-F2 for ozone concentrations

3.4.4 Regionalization of the study area

Based on the results of individual and variables projections on the factorial plane F1-F2, the study area can be subdivided (**Figure 9-a**) :

- in 4 regions for ozone concentration 6h, 12h and 18h :

Region 1 : consists of **A7** (in green).This region has low ozone concentrations during the months of January, June, July and August.

Region 2 : consists of **G3** and **G4** (in blue). This region has a higher concentration of ozone during the months of January, June, July and August.

Region 3 : consists of **A1**, A2, **A3**, **A4**, **A5**, **A6**, **B1**, **B2**, **B3**, **B4**, **B5**, **B6**, **B7**, **C1**, **C2**, **C3**, **D1, D2**, **D3**, **D4**, **D5**, **D6**, **D7**, **E1**, **E2**, **E3**, **E4**, **E5**, **E6**, **F1**, **F2**, **F3**, **F4**, **F5**, **F6**, **G1**, **G2**, **G5**, **G6**, **G7, H1, H2**, **H3**, **H4**, **H5**, **H6**, **H7**, **I1**, **I2**, **I3**, **I4**, **I5**, **I6** and **I7** (in purple). This region has no particular behavior with respect to

ozone concentrations.

Region 4 : consists of **E7** and **F7** (in red). This region has higher concentrations of ozone during the months of September, October and November.

- in 3 regions for ozone concentration 0h (**Figure 9-b**):

Region 1 : consists of **A7** (in green). This region has low ozone concentrations during January, June, July and August.

Region 2 : consists of **G3** and **G4** (in blue). This region has higher ozone concentrations during January, June, July and August.

Region 3 : consists of **A1**, A**2**, **A3**, **A4**, **A5**, **A6**, **B1**, **B2**, **B3**, **B4**, **B5**, **B6**, **B7**, **C1**, **C2**, **C3**, **D1, D2**, **D3**, **D4**, **D5**, **D6**, **D7**, **E1**, **E2**, **E3**, **E4**, **E5**, **E6**, **E7**, **F1**, **F2**, **F3**, **F4**, **F5**, **F6**, **F7**, **G1**, **G2**, **G5**, **G6**, **G7, H1, H2**, **H3**, **H4**, **H5**, **H6**, **H7**, **I1**, **I2**, **I3**, **I4**, **I5**, **I6** and **I7** (in purple). This region has no particular behavior with respect to ozone concentrations.

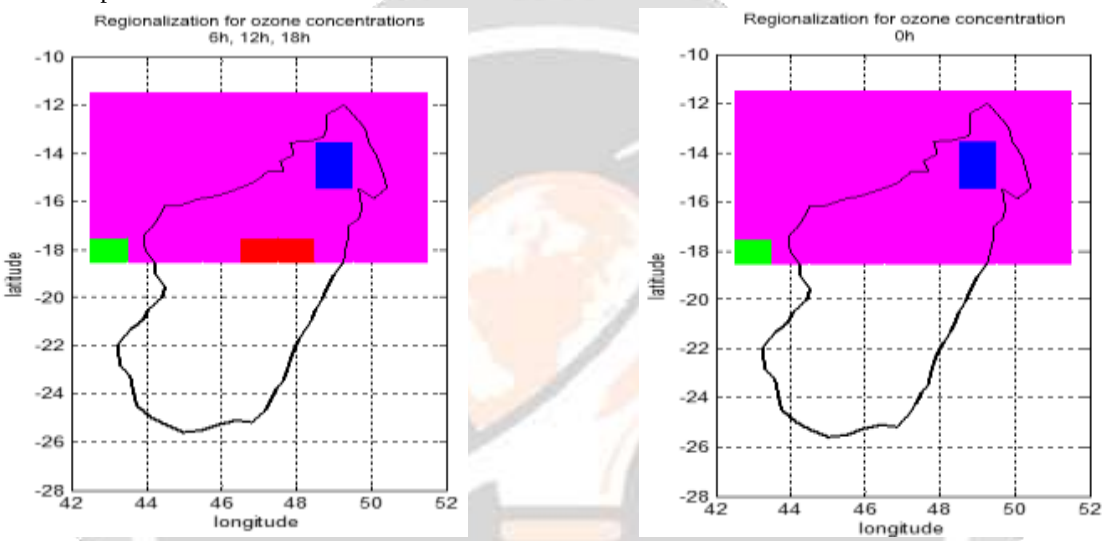

Figure 9-a **Figure 9-b**

Figure 9 : distribution of regions with similar ozone concentrations

3.5 Prediction of ozone concentration evolution in each region

Figure 10 represents the prediction of the ozone concentration in regions 1,2 and 3 by ARIMA method. Initially, the differences between the forecast and the ozone data 0h are (in percent):

Regions	Difference (%)
Region 1	0,23%
Region 2	1,95%
Region 3	0,05%

From 2023 to 2044, the annual ozone concentration in region 1 and 2 would stabilize around 5.625×10^{-3} $kg.m^{-2}$
The annual concentration of ozone 0h in region 3 would oscillate almost periodically 13 years period.

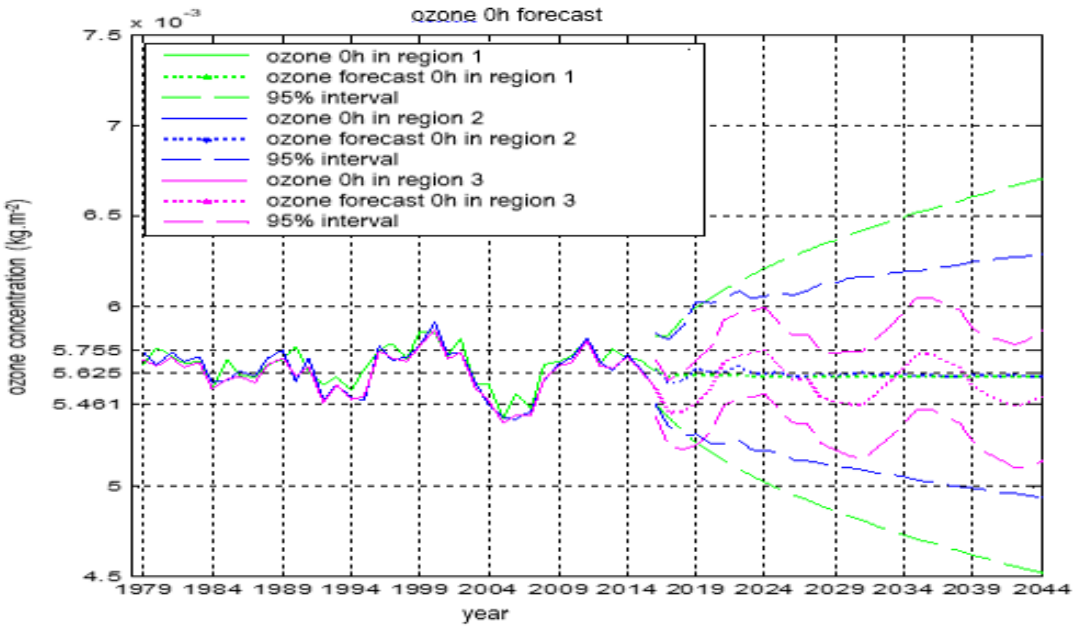

Figure 10: prediction of ozone 0h concentration evolution

Figure 11 represents the prediction of the concentration of ozone 6h in regions 1, 2, 3 and 4. Initially, the differences between the forecast and the ozone data 6h are (in percent):

Regions	Difference (%)
Region 1	-0,05
Region 2	1,86
Region 3	0,91
Region 4	1,74

The annual concentration of ozone 6h in Region 1 would be subject to an almost periodic 11 years amortized oscillation.

Annual ozone 6h concentrations in region 2 and 4 would also be subject to an almost amortized oscillation periodic of 11 years but of smaller amplitude.

The annual 6h ozone concentration in Region 3 would decrease from 2021 to 2044 but remain above its minimum $5{,}473 \times 10^{-3}$ $kg.m^{-2}$ in 2006.

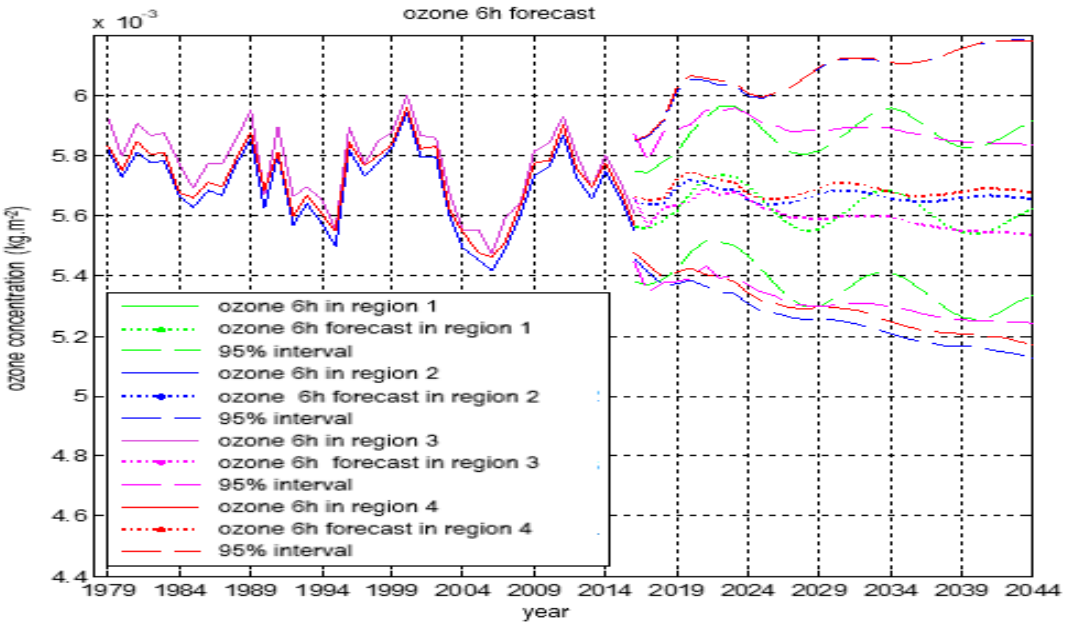

Figure 11: prediction of ozone 6h concentration evolution

La **Figure 12** represents the prediction of the concentration of ozone 12h in regions 1, 2, 3 and 4. Initially, the differences between the forecast and the ozone data 12h are (in percent):

Regions	Difference (%)
Region 1	0,16
Region 2	1,77
Region 3	0,82
Region 4	1,71

Annual ozone 12h concentrations in Region 2 and 4 would be subject to a weakly amortized periodic oscillation of 11 years period.

The annual 12h ozone concentration in Region 3 would decrease from 2021 to 2044, but remain above its minimum 5.466×10^{-3} kg.m^{-2} in 2006.

The annual ozone 12h concentration in region 1 would remain constant very close to 5.586×10^{-3} kg.m^{-2}

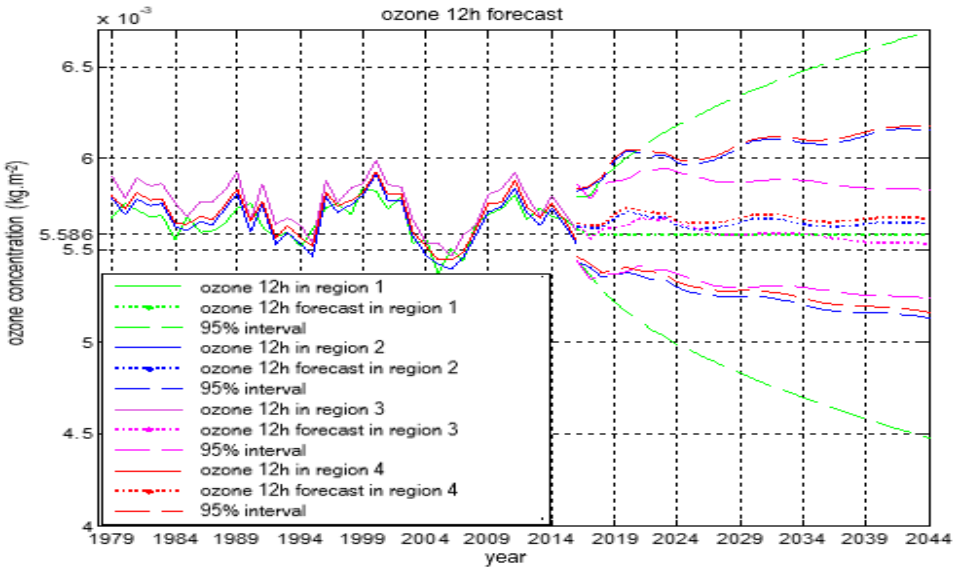

Figure 12: prediction of ozone 12h concentration evolution

La **Figure 13** represents the prediction of the concentration of ozone 18h in regions 1, 2, 3 and 4. Initially, the differences between the forecast and the ozone data 18h are (in percent):

Regions	Difference (%)
Region 1	0,84
Region 2	1,74
Region 3	-1,09
Region 4	2,02

The annual ozone 18h concentration in region 3 would oscillate almost periodically 12 years.
The annual ozone 18h concentration in Region 2 would fluctuate almost periodically over a 10 years period but at low amplitude.
The annual ozone 18h concentration in Region 4 would remain constant very close to 5.659 $x10^{-3}$ $kg.m^{-2}$ from 2034 to 2044.
The annual ozone 18h concentration in Region 1 would remain constant very close to 5.68 $x10^{-3}$ $kg.m^{-2}$ from 2033 to 2044.

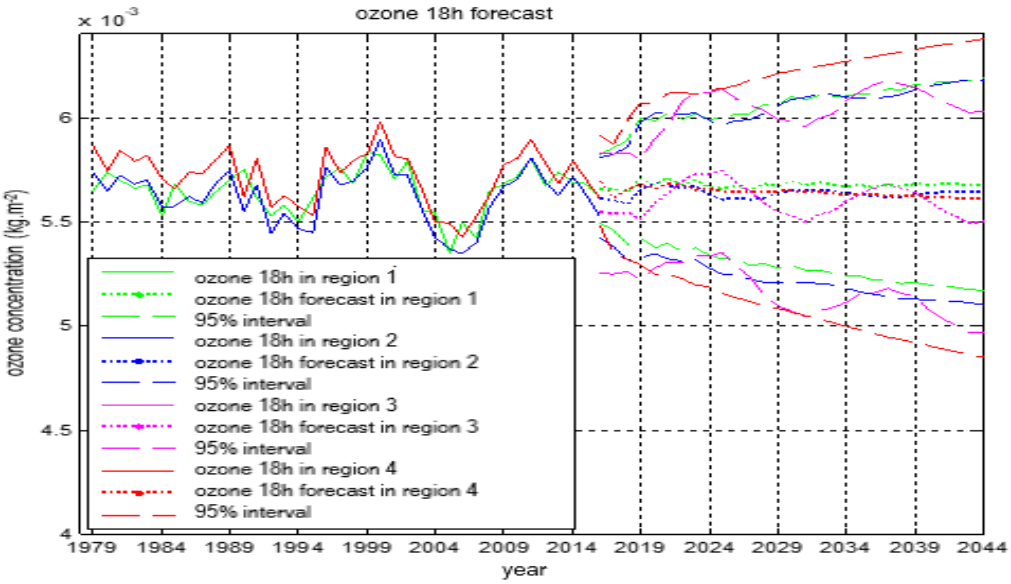

Figure 13: prediction of ozone 18h concentration evolution

4. CONCLUSIONS

During the study period from 1979 to 2016, the ozone concentration in the northern part of Madagascar showed no significant trend. This period of study was characterized by an almost periodic alternation of surplus and deficit of ozone concentrations of period 4 years between 1979 and 1995, period 6 years between 1996 and 2014. The greatest excess ($+2{,}56x10^{-4}$ $kg.m^{-2}$) occurred in 2000 observed for the ozone concentration 18h and the largest deficit ($-2.7x10^{-4}$ $kg.m^{-2}$) in 2005 observed for ozone concentration 0h.

The regionalization of the study area by principal component analysis showed that the area can be subdivided into three regions for common variations concentrations of ozone 0h, 6h, 12h and 18h and a fourth region is added for common variations concentrations ozone 6h, 12h and 18h :

region 1 : region of low ozone concentration during the months of January, June, July and August.
region 2 : regions with higher ozone concentrations during January, June, July and August.
region 3 : region that has no particular behavior with respect to ozone concentrations.
region 4 : region of highest concentrations of ozone during the months of September, October and November.

The prediction of the evolution of ozone concentrations by the ARIMA method showed that there would be a quasi-periodic oscillation for some regions, a constant value or a decrease for others but no threat of danger until 2044.

5. REFERENCES

[1] N. Croiset, B. Lopez (BRGM), Outil d'analyse statistique des séries temporelles d'évolution de la qualité des eaux souterraines, Manuel d'utilisation, Rapport final, pp.18-19

[2] P. Besse www.math. univ-toulouse.fr/besse, M2 MASS, TP4 : Introduction au logiciel SAS Procédures statistiques multivariées : Analyse en Composantes Principales. Pages 1, 2.

[3] C.DUBY, S ROBIN ; Analyse composantes principale, juillet 2006. Pages 4,5.

[4] Aimé KOUDOU et al, CONTRIBUTION DE L'ANALYSE EN COMPOSANTES PRINCIPALES A LA REGIONALISATION DES PLUIES DU BASSIN VERSANT DU N'ZI, CENTRE DE LA COTE D'IVOIRE, 2015. Page 162.

[5] Ali Kouani, S. El Jamali et M.Talbi, Analyse en Composantes principales, Une méthode factorielle pour traiter les données didactique, février 2007. Page 3.

[6] ADD3-MAB, D-interpretation d'une ACP, 2011.Papes 4, 29.

[7] Jean-Marc Labatte, jean-marc.Labatte@univ-angers.fr, Analyse des données M2, consulté le 17 Février 2017.

[8] www.agroparistech.fr/IMG/pdf/Polychro.pdf, consulté le 5 Septembre 2018

[9] lacote.ensae.net/SE206/Cours/Joachim.Connault.pdf